Time- and Frequency-Domain-Spread Generalized Multicarrier DS-CDMA Using Subspace-Based Blind and Group-Blind Space–Time Multiuser Detection

Bin Hu, Lie-Liang Yang, and Lajos Hanzo

***Abstract*—Subspace-based blind and group-blind space–time (ST) multiuser detection (MUD) is invoked for a smart-antenna-aided generalized multicarrier direct-sequence code-division multiple-access (MC DS-CDMA) system communicating over a dispersive ST Rayleigh fading channel, where the channel estimates are attained by using subspace-based blind techniques. Smart antennas are employed to provide increased degrees of freedom and, hence, to improve both the attainable single-user performance and the multiuser capacity. Furthermore, two adaptive subspace-tracking algorithms, i.e., the Projection Approximation Subspace-Tracking deflation (PASTd) algorithm and the Noise-Averaged Hermitian–Jacobi Fast Subspace Tracking (NAHJ-FST) algorithm, are employed for the sake of reducing the computational complexity imposed by eigenvalue decomposition. When employing the NAHJ-FST algorithm, the group-blind MUD employing an antenna array having $M = 2$ elements exposed to uncorrelated fading achieved a 4.2-dB signal-to-noise-ratio (SNR) gain at a bit error rate (BER) of 10^{-4} compared with that employing a single antenna, which is an explicit benefit of its increased computational complexity.**

***Index Terms*—Blind multiuser detection, frequency-domain spreading, generalized MC-CDMA, group-blind multiuser detection, MUD, time-domain spreading.**

I. Introduction

Recently, a considerable amount of research has been devoted to multiuser detection (MUD) [1]–[5], which is capable of eliminating the effects of multiuser interference and, hence, has the potential of increasing the capacity of code-division multiple-access (CDMA) systems. The optimum MUD proposed by Verdu [1] is capable of attaining a near-single-user performance at the expense of an exponentially increasing complexity as a function of increasing the number of users supported. A training-sequence-based adaptive MUD was introduced in [5]–[8], which requires the knowledge of the signature waveform and the timing information of the desired user, but no other knowledge is needed. Contrary to the training-sequence-based adaptive MUD, the minimum-output-energy (MOE)-based blind adaptive MUD [2] requires no training sequence and, hence, achieves an increased spectrum efficiency although its performance is suboptimum in the high-signal-to-noise ratio (SNR) region. In [3] and [9], Wang and Poor proposed a novel blind MUD for single-carrier direct-sequence code-division multiple-access (DS-CDMA) systems based on the philosophy of signal subspace estimation, which benefits from a lower computational complexity and a better performance, compared with the MOE-based blind MUD. Group-blind MUDs having prior knowledge of all the signature waveforms of the intracell users were then proposed in [4] for the uplink of a single-carrier DS-CDMA system, which exhibited a significant performance improvement over that of the blind MUDs advocated in [3] and [9]. Furthermore, in [10], a subspace-based minimum mean square error (MMSE) receiver was proposed for a multicarrier DS-CDMA (MC DS-CDMA) system, where the orthogonality between the noise subspace and the desired signal vector was exploited to blindly extract both the required timing and the channel information.

In this contribution, subspace-based blind and group-blind space–time (ST) MUDs are invoked as joint ST frequency-domain (FD) MUDs for the smart-antenna-aided generalized MC DS-CDMA system in [11] since subspace-based estimation techniques [3], [9], [10] are capable of extracting the required channel estimates. More explicitly, the novelty of this contribution is that we combine the benefits of subspace-based blind and group-blind ST MUDs with those of the smart-antenna-aided generalized MC DS-CDMA system in [11] to improve the achievable performance of the system by jointly performing MUD in the ST FD while achieving both frequency and spatial diversity.

The rationale of the proposed solution is multifold. First, a potentially high interference is imposed by the channel-sounding pilot of CDMA systems, which is necessary to estimate all the multi-input–multi-output links. Unfortunately, this channel-sounding overhead erodes the gains attained by the introduction of smart antennas. Hence, it is of future benefit for next-generation systems to develop powerful joint blind or group-blind data detection and channel estimation techniques. Second, in recent years, the community has turned to investigating cooperative wireless systems, where it would be unreasonable to expect that the relay stations provide pilot signals for assisting other mobiles in their channel-estimation efforts. As a potential option, the relay stations may employ similar blind or group-blind techniques to jointly detect a few users' signals to support them by relaying. Third, the joint time-domain (TD) and FD spreading has substantial benefits, which next-generation systems are expected to exploit. More explicitly, let us, for example, consider a system that has to support 64 users. This would impose a high MUD complexity, which is an exponentially increasing function of the code length. Hence, it is significantly more efficient to use a spreading factor of 8 in both the TD and the FD, resulting in two low-complexity MUD steps. Furthermore, this 2-D spreading regime has the benefit of providing both TD and FD diversity.

The rest of this paper has the following structure. In Section II, the philosophy of a generalized MC DS-CDMA system employing smart antennas will be described and characterized. Then, a subspace-based blind-channel-estimation technique is invoked for the smart-antenna-aided generalized MC DS-CDMA system considered in Section III. Section IV develops subspace-based blind and group-blind ST MUDs in the context of the smart-antenna-aided generalized MC DS-CDMA system. Two low-complexity subspace-tracking algorithms, i.e., the Projection Approximation Subspace-Tracking deflation (PASTd) algorithm and the Noise-Averaged Hermitian–Jacobi Fast Subspace Tracking (NAHJ-FST) algorithm, are investigated in Section V. The attainable performance of these MUDs is comparatively studied in Section VI. Finally, we provide our conclusions in Section VII.

II. System Model

The transmitter of the generalized MC DS-CDMA system is shown in Fig. 1. At the transmitter side, the binary data stream $b_k(t)$ having a bit duration of T_b is spread using an N-chip TD direct-sequence (DS) spreading waveform $c_k(t)$, and the chip duration was $T_c = T_b/N$. The DS-spread signals are simultaneously modulated using binary phase-shift keying and then spread using an orthogonal FD spreading sequence $\mathbf{c}'_k = [c'_{k,0}, c'_{k,1}, \ldots, c'_{k,V-1}]$ of length V, where we have $\mathbf{c}'_k \cdot \mathbf{c}'^H_l = \delta_{kl}$ ($\delta_{kl} = 1$ if $k = l$ and $\delta_{kl} = 0$ if $k \neq l$). In this section, we assume that orthogonal frequency-division multiplexing (OFDM)

Manuscript received February 28, 2006; revised August 19, 2007, December 14, 2007, and December 23, 2007. This work was supported in part by the Engineering and Physical Sciences Research Council, U.K., and in part by the European Union under the Optimix Project. The review of this paper was coordinated by Prof. Y. Ma.

The authors are with the School of Electronics and Computer Science, University of Southampton, SO17 1BJ Southampton, U.K.

Digital Object Identifier 10.1109/TVT.2008.917231

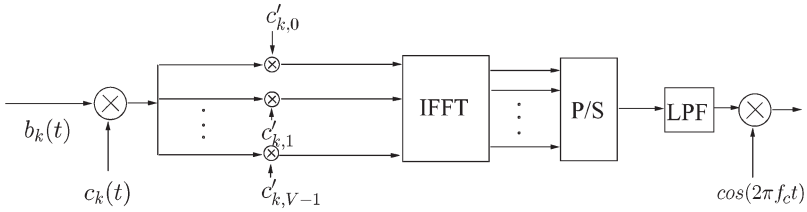

Fig. 1. Transmitter schematic of MC DS-CDMA using both N-chip TD and V-chip FD spreading.

using V subcarriers was invoked [12] and that the OFDM-chip duration was $T_c' = T_b/NV$. After inverse fast Fourier transform (FFT) and parallel-to-serial conversion [11], a sufficiently long cyclic prefix is inserted in the OFDM symbol for the sake of compensating for the delay-spread-induced intersymbol interference (ISI) imposed by the dispersive channel [12]. For analytical tractability, it is assumed that the multipath fading channel has L paths for all the K users. Upon assuming that, at the base station, there are M number of receiver antenna elements (AEs) and that the channel encountered is time invariant during three consecutive bits, the spatio-temporal channel impulse response (CIR) $h_{km}(t)$ between the kth user and the mth AE can be expressed as

$$h_{km}(t) = \sum_{l=0}^{L-1} h_{km,l}\delta(t - lT_{c'}) \tag{1}$$

where $h_{km,l}$ is the complex-valued channel gain experienced by the signal of the kth user in the lth path impinging on the mth AE, which obeys Rayleigh fading.

At each AE, the TD samples of the received signal corresponding to the cyclic prefix are first removed, and the V-point FFT is invoked to demodulate the remaining V samples and to generate the demodulated subcarrier signals in the FD [12]. Consequently, the received signal can be written as $\mathbf{r}(t) = [\mathbf{r}_0^T(t), \mathbf{r}_1^T(t), \ldots, \mathbf{r}_{M-1}^T(t)]^T$, where $\mathbf{r}_m(t) \in \mathcal{R}^V$ is given by

$$\mathbf{r}_m(t) = \sum_{k=1}^{K} \mathbf{C}'_k \mathbf{H}_{km} \sum_{i=0}^{M_F-1} A_k b_k[i] c_k(t - iT_b - \tau_k) + \mathbf{n}_m(t) \tag{2}$$

and $\mathbf{H}_{km} = [H_{km,0}, H_{km,1}, \ldots, H_{km,V-1}]^T$ denotes the FD channel transfer function (FDCTF) between the kth user and the mth AE. In (2), M_F is the length of the transmitted data frame, whereas A_k, $\{b_k[i]\}$, and $0 \le \tau_k < T_b$ represent the received signal amplitude, symbol stream, and the delay of the kth user, respectively. The spreading sequence $c_k(t) = \sum_{j=0}^{N-1} c_k(j)\psi(t - jT_c)$ in (2) denotes the signature waveform of the kth user, where $c_k(j)$ assumes values of $+1$ or -1 with equal probability, and $\psi(t)$ is a normalized chip waveform of duration T_c. Furthermore, in (2), $\mathbf{C}'_k = \mathrm{diag}\{\mathbf{c}'_k\}$, and $\mathbf{n}_m(t)$ represents the additive white Gaussian noise (AWGN) vector associated with the covariance matrix of $\sigma^2\mathbf{I}_V$, where $\mathbf{I}_V$ denotes the $(V \times V)$-dimensional identity matrix. Since we assume that a sufficiently long cyclic prefix was inserted and that we have $V \ge L$, every subcarrier experiences flat fading; hence, no OFDM ISI is incurred. Therefore, the FDCTF $\mathbf{H}_{km}$ in (2) can be expressed as the V-point discrete Fourier transform (DFT) of $\mathbf{h}_{km} = [h_{km,0}, \ldots, h_{km,L-1}]^T$ in the form of $\mathbf{H}_{km} = \mathbf{F}_L \cdot \mathbf{h}_{km}$, where $\mathbf{F}_L$ is a $(V \times L)$-dimensional matrix, which is given by the first L columns of the DFT matrix $\mathbf{F}$, which is formulated as

$$\mathbf{F} = \begin{pmatrix} 1 & 1 & \cdots & 1 \\ 1 & e^{-j2\pi/V} & \cdots & e^{-j2\pi(V-1)/V} \\ \vdots & \vdots & \ddots & \vdots \\ 1 & e^{-j2\pi(V-1)/V} & \cdots & e^{-j2\pi(V-1)(V-1)/V} \end{pmatrix}.$$

A set of $M \cdot V$ chip-matched filters is used to sample the received signal $\mathbf{r}(t)$ at a rate of $1/T_c$. Since the delay spread is often assumed to be one symbol interval with a duration of T_b in practical CDMA systems [9], we observe the chip-matched filter outputs for a duration of $2T_b$, so that, despite the channel-induced ISI, a completely interference-free symbol of the desired user is guaranteed to be observed. Hence, the nth received signal sample of the vth chip-matched filter corresponding to the mth AE during the lth symbol has the form of

$$r_{m,v}[l,n] = r_{m,v}(lT_b + nT_c) = \sum_{k=1}^{K} y_{km,v}[l,n] + n_{m,v}[l,n] \tag{3}$$

where $n_{m,v}[l,n]$ is the AWGN component, and

$$y_{km,v}[l,n] = A_k H_{km,v} c'_{k,v} \sum_{i=0}^{M_F-1} \sum_{j=0}^{N-1} b_k[i] c_k(j) \times \hat{\psi}\left((lN + n - j - iN)T_c - \tau_k\right) \tag{4}$$

is the component due to the kth user's signal received at the mth AE. The function $\hat{\psi}(t) = \int_{-\infty}^{\infty} \psi(s)\psi^*(s-t)ds$ in (4) represents the chip waveform output of the chip-matched filter.

Let us define the $2N$-dimensional vectors

$$\bar{\mathbf{r}}_{m,v}[l] = [r_{m,v}[l,0], \ldots, r_{m,v}[l,2N-1]]^T$$
$$\bar{\mathbf{n}}_{m,v}[l] = [n_{m,v}[l,0], \ldots, n_{m,v}[l,2N-1]]^T$$
$$\bar{\mathbf{y}}_{km,v}[l] = [y_{km,v}[l,0], \ldots, y_{km,v}[l,2N-1]]^T.$$

By concatenating the VM vectors corresponding to the V subcarriers and the M AEs, we obtain the following $2NVM$-dimensional vectors:

$$\mathbf{r}[l] = \underbrace{\left[\bar{\mathbf{r}}_{00}^T[l], \ldots, \bar{\mathbf{r}}_{(M-1)(V-1)}^T[l]\right]^T}_{VM}$$
$$\mathbf{n}[l] = \underbrace{\left[\bar{\mathbf{n}}_{00}^T[l], \ldots, \bar{\mathbf{n}}_{(M-1)(V-1)}^T[l]\right]^T}_{VM} \tag{5}$$
$$\mathbf{y}_k[l] = \underbrace{\left[\bar{\mathbf{y}}_{k0,0}^T[l], \ldots, \bar{\mathbf{y}}_{k(M-1),V-1}^T[l]\right]^T}_{VM}.$$

Hence, (3) can be rewritten as

$$\mathbf{r}[l] = \sum_{k=1}^{K} \mathbf{y}_k[l] + \mathbf{n}[l]. \tag{6}$$

Without loss of generality, let $b_k[l]$ represent the specific bit of the kth user that completely falls within the lth symbol period, and for simplicity, let us normalize the value of $\tau_k \in [0, T_b)$ to the chip duration T_c. Therefore, we have $\tau_k = n_k T_c$, where n_k is an integer between

zero and $N-1$. Let $\mathbf{c}_k = [c_k(0), c_k(1), \ldots, c_k(N-1), \underbrace{0, \ldots, 0}_{N}]^T$ denote a vector of length $2N$ that consists of the N elements of the spreading sequence of the kth user followed by N zeros. Following the notation in [8], we define $\mathbf{T}_L$ and $\mathbf{T}_R$ as the acyclic left- and right-shift operator processing vectors of length $2N$, respectively. Then, we use $\mathbf{T}_L^n$ and $\mathbf{T}_R^n$ to denote n applications of these operators, resulting in n left and right shifts, respectively. Based on these operators, we define $\underline{\mathbf{v}}_k^{-1} = \mathbf{T}_L^{N-n_k}\mathbf{c}_k$, $\underline{\mathbf{v}}_k^0 = \mathbf{T}_R^{n_k}\mathbf{c}_k$ and $\underline{\mathbf{v}}_k^1 = \mathbf{T}_R^{N+n_k}\mathbf{c}_k$.

For each asynchronous user, three-consecutive-bit intervals overlap with a given observation interval of length $2T_b$. Furthermore, since the system is chip asynchronous, two adjacent chips contribute to each chip sample. The contribution of the kth user $\mathbf{y}_k[l]$ to the received vector $\mathbf{r}[l] \in \mathcal{R}^{2NVM}$ in (6) for the lth symbol is therefore given by

$$\mathbf{y}_k[l] = \check{\mathbf{D}}_k \left(b_k[l-1]\check{\mathbf{v}}_k^{-1} + b_k[l]\check{\mathbf{v}}_k^0 + b_k[l+1]\check{\mathbf{v}}_k^1 \right) \tag{7}$$

where

$$\check{\mathbf{D}}_k = \operatorname{diag}\left(\mathbf{D}_{k0}, \mathbf{D}_{k1}, \ldots, \mathbf{D}_{k(M-1)}\right)$$

is a $(2NVM \times 2NVM)$-dimensional matrix, and

$$\mathbf{D}_{km} = \operatorname{diag}\left(A_k H_{km,0} c'_{k,0}, \ldots A_k H_{km,0} c'_{k,0}, \ldots A_k H_{km,V-1} c'_{k,V-1}, \ldots, A_k H_{km,V-1} c'_{k,V-1}\right).$$

Furthermore, we have $\check{\mathbf{v}}_k^{-1} = [\underbrace{(\underline{\mathbf{v}}_k^{-1})^T, \ldots, (\underline{\mathbf{v}}_k^{-1})^T}_{VM}]^T$, $\check{\mathbf{v}}_k^0 = [\underbrace{(\underline{\mathbf{v}}_k^0)^T, \ldots, (\underline{\mathbf{v}}_k^0)^T}_{VM}]^T$, and $\check{\mathbf{v}}_k^1 = [\underbrace{(\underline{\mathbf{v}}_k^1)^T, \ldots, (\underline{\mathbf{v}}_k^1)^T}_{VM}]^T$. Upon substituting (7) into (6), we arrive at

$$\mathbf{r}[l] = \check{\mathbf{D}}_1 b_1[l]\check{\mathbf{v}}_1^0 + \sum_{k=1}^{K} \check{\mathbf{D}}_k \left(b_k[l-1]\check{\mathbf{v}}_k^{-1} + b_k[l+1]\check{\mathbf{v}}_k^1 \right) + \sum_{k=2}^{K} \check{\mathbf{D}}_k b_k[l]\check{\mathbf{v}}_k^0 + \mathbf{n}[l] \tag{8}$$

and for notational convenience, (8) can be rewritten as follows by using the equivalent synchronous model described in [8]:

$$\mathbf{r}[l] = b_1[l]\check{\mathbf{p}}_1 + \sum_{j=2}^{J} b_j[l]\check{\mathbf{p}}_j + \mathbf{n}[l] \tag{9}$$

where $b_1[l]$ is the desired bit, $\check{\mathbf{p}}_1 = \check{\mathbf{D}}_1\check{\mathbf{v}}_1^0$, and the remaining vectors correspond to the ISI and MAI vectors in (8). Note that we have $2K \leq J \leq 3K$.

III. Blind Channel Estimation

The eigenvalue decomposition (EVD) of the autocorrelation matrix $\mathbf{R}$ of the received MC DS-CDMA signal vector $\mathbf{r}$ is given by [4]

$$\begin{aligned}\mathbf{R} &= E\{\mathbf{r}\mathbf{r}^H\} = \check{\mathbf{P}}\check{\mathbf{P}}^H + \sigma^2 I_{2NVM} \\ &= \mathbf{U}\mathbf{\Lambda}\mathbf{U}^H = [\mathbf{U}_s \quad \mathbf{U}_n] \begin{bmatrix} \mathbf{\Lambda}_s & 0 \\ 0 & \mathbf{\Lambda}_n \end{bmatrix} \begin{bmatrix} \mathbf{U}_s^H \\ \mathbf{U}_n^H \end{bmatrix}\end{aligned} \tag{10}$$

where we have $\check{\mathbf{P}} = [\check{\mathbf{p}}_1, \ldots, \check{\mathbf{p}}_J]$, $\mathbf{U} = [\mathbf{U}_s \quad \mathbf{U}_n]$, and $\mathbf{\Lambda} = \operatorname{diag}(\mathbf{\Lambda}_s, \mathbf{\Lambda}_n)$. Without loss of generality, we have $\mathbf{r} = \mathbf{r}[l]$, and we assume that the vectors $\check{\mathbf{p}}_1, \ldots, \check{\mathbf{p}}_J$ are linearly independent and that $J < 2NVM$. Hence, matrix $\mathbf{P}$ is a "tall" matrix having a rank of $\operatorname{rank}(\mathbf{P}) = \operatorname{rank}(\mathbf{P}\mathbf{P}^H) = J$, and $\mathbf{\Lambda}_s = \operatorname{diag}\{\lambda_1, \ldots, \lambda_J\}$ contains the largest J eigenvalues of the received signal's autocorrelation matrix $\mathbf{R}$. Contrary to the *signal space* $\mathbf{U}_s = [\mathbf{u}_1, \ldots, \mathbf{u}_J]$, the *noise space* $\mathbf{U}_n = [\mathbf{u}_{J+1}, \ldots, \mathbf{u}_{2NVM}]$ contains the $(2NVM - J)$ orthogonal eigenvectors corresponding to the smallest eigenvalues σ^2 in $\mathbf{\Lambda}_n$.

As shown in [4] and [9], the ML-dimensional CIR vector $\mathbf{h}_1 = [\mathbf{h}_{10}^T, \ldots, \mathbf{h}_{1m}^T, \ldots, \mathbf{h}_{1(M-1)}^T]$ of the desired user can be estimated by exploiting the orthogonality between the signal subspace and the noise space. More specifically, $\mathbf{U}_n$ is orthogonal to the column space of $\check{\mathbf{P}}$, and $\check{\mathbf{p}}_1$ represents the column space of $\check{\mathbf{P}}$. Therefore, we have

$$\mathbf{U}_n^H\check{\mathbf{p}}_1 = \mathbf{U}_n^H\check{\mathbf{V}}_1^0\check{\mathbf{d}}_1 = A_1\mathbf{U}_n^H\check{\mathbf{V}}_1^0\check{\mathbf{C}}_1'\check{\mathbf{F}}_L\mathbf{h}_1 = 0 \tag{11}$$

where we have the $(2NVM \times VM)$-dimensional TD spreading code matrix $\check{\mathbf{V}}_1^0 = \operatorname{diag}(\underline{\mathbf{v}}_1^0, \ldots, \underline{\mathbf{v}}_1^0)$, the $(VM \times VM)$-dimensional FD spreading code matrix $\check{\mathbf{C}}_1' = \operatorname{diag}(\mathbf{C}_1', \ldots, \mathbf{C}_1')$, and the $(MV \times ML)$-dimensional matrix $\check{\mathbf{F}}_L = \operatorname{diag}(\mathbf{F}_L, \ldots, \mathbf{F}_L)$.

The estimate $\bar{\mathbf{h}}_1$ of the CIR vector $\mathbf{h}_1$ can be generated by computing the minimum eigenvector of the matrix $\check{\mathbf{F}}_L^H\check{\mathbf{C}}_1'^H(\check{\mathbf{V}}_1^0)^H\mathbf{U}_n\mathbf{U}_n^H\check{\mathbf{V}}_1^0\check{\mathbf{C}}_1'\check{\mathbf{F}}_L$. The necessary condition for such an estimate to be unique is that we have $J \leq 2NVM - LM$. For the worst-case scenario of $J = 3K$, a necessary condition imposed on the number of users for the sake of uniquely determining $\mathbf{h}_1$ is then $K \leq ((2NV - L)M/3)$. When we have $M \geq 2$, the number of users supported can be $K = NV$, provided that the condition of $((2M-3)NV/M) \geq L$ is met, which can readily be satisfied by appropriately choosing M, N, and V. Compared with the generalized MC DS-CDMA system using a single antenna, the smart-antenna-aided system is capable of supporting more users because, generally speaking, increasing the number of AEs has the potential of providing a higher degree of freedom and, hence, the capability of improving both the achievable system performance and the user capacity. Furthermore, with the aid of an appropriately chosen cyclic prefix, we can remove the phase ambiguity encountered in the channel-estimation process by using the techniques proposed in [13].

If the value of τ_1 is not available, joint timing and channel estimation must be carried out for the desired user, which is summarized here.

1) Hypothesize a value for $\tau_1 < T_b$, and construct matrix $\mathbf{V}_1^0(\tau_1)$ based on this hypothesized value.
2) Obtain the best estimate $\bar{\mathbf{h}}_1(\tau_1)$ by computing the minimum eigenvector of matrix $\mathbf{F}_L^H\mathbf{C}_1'^H(\mathbf{V}_1^0)^H\mathbf{U}_n\mathbf{U}_n^H\mathbf{V}_1^0\mathbf{C}_1'\mathbf{F}_L$ for this value of τ_1.
3) Repeat Steps 1) and 2) for different values of τ_1.
4) Attain the best timing estimate $\bar{\tau}_1$ by solving the minimization problem in [10], i.e.,

$$\begin{aligned}\bar{\tau}_1 &= \arg\min_{\tau_1 \in [0, T_b)} \Omega(\tau_1) \\ &= \arg\min_{\tau_1 \in [0, T_b)} \frac{\left\|\mathbf{U}_n^H\mathbf{V}_1^0(\tau_1)\mathbf{C}_1'\mathbf{F}_L\bar{\mathbf{h}}_1(\tau_1)\right\|^2}{\left\|\mathbf{V}_1^0(\tau_1)\mathbf{C}_1'\mathbf{F}_L\bar{\mathbf{h}}_1(\tau_1)\right\|^2}.\end{aligned} \tag{12}$$

5) Arrive at the best channel estimate $\bar{\mathbf{h}}_1(\bar{\tau}_1)$ based on $\bar{\tau}_1$.

In practice, we have to quantize the infinite number of possible hypothesized values of τ_1 in the interval $[0, T_b]$ to a finite set. Since the optimization problem in (12) is 1-D, not all choices of the pair $(\tau_1, \mathbf{h}_1)$ are legitimate. The procedure previously described leads to the best estimate $\bar{\mathbf{h}}_1(\tau_1)$ for a specific hypothesized value of τ_1. Therefore, the search space is substantially reduced, rendering the aforementioned method more practical. Furthermore, since $\Omega(\tau_1) = (\|\mathbf{U}_n^H\mathbf{V}_1^0(\tau_1)\mathbf{C}_1'\mathbf{F}_L\bar{\mathbf{h}}_1(\tau_1)\|^2 / \|\mathbf{V}_1^0(\tau_1)\mathbf{C}_1'\mathbf{F}_L\bar{\mathbf{h}}_1(\tau_1)\|^2)$ is a continuous function of τ_1, it must have a minimum within the closed interval $[0, T_b]$, which guarantees the optimal choice of τ_1 that minimizes the cost function, provided that we search on a sufficiently fine grid.

IV. Blind and Group-Blind MUD

Given the prior knowledge of the desired user's signature waveform, the linear MMSE MUD weights $\mathbf{w}_1 = \mathbf{m}_1$ can be expressed in terms of the signal subspace components $\mathbf{U}_s$, $\mathbf{\Lambda}_s$, and σ^2 and the estimated composite signature waveform $\bar{\mathbf{p}}_1 = \check{\mathbf{V}}_1^0(\tau_1)\check{\mathbf{C}}_1'\check{\mathbf{F}}_L\bar{\mathbf{h}}_1$ as

$$\mathbf{m}_1 = \mathbf{U}_s\mathbf{\Lambda}_s^{-1}\mathbf{U}_s^H\bar{\mathbf{p}}_1 \tag{13}$$

which is obtained by solving the following optimization problem [4]:

$$\mathbf{m}_1 = \arg\min_{\mathbf{w}\in\mathcal{R}^{2NVM}} E\left\{|b_1 - \mathbf{w}^H\mathbf{r}|^2\right\} = \mathbf{R}^{-1}\bar{\mathbf{p}}_1. \tag{14}$$

Furthermore, the so-called form-II linear hybrid group-blind MUD $\bar{\mathbf{w}}_1$ [4], which exploits the knowledge of a group of $\tilde{K}$ composite signature waveforms corresponding to $\tilde{K}(\tilde{K} \leq K)$ intracell users, is given by the solution of the following constrained optimization problem [4]:

$$\bar{\mathbf{w}}_1 = \arg\min_{\mathbf{w}_1\in range(\mathbf{P})} E\left\{|b_1 - \mathbf{w}_1^H\mathbf{r}|^2\right\} \tag{15}$$

subject to $\mathbf{w}_1^H\tilde{\mathbf{P}} = \mathbf{1}_1^T$, where $\mathbf{1}_1$ is a $\tilde{J}$-dimensional vector having all-zero elements, except for the first element, which is one, and $\tilde{\mathbf{P}} = [\bar{\mathbf{p}}_1, \ldots, \bar{\mathbf{p}}_{\tilde{J}}]$ is a $(2NVM \times \tilde{J})$-dimensional matrix constructed based on the estimated CIRs, the timing information, and the time–frequency-domain spreading signature waveforms of all the $\tilde{K}$ intracell users. Hence, we have $2\tilde{K} \leq \tilde{J} \leq 3\tilde{K}$. Using the method of Lagrange multipliers [4] in (15), we obtain the form-II linear hybrid group-blind MUD's weight vector in the form of [4]

$$\bar{\mathbf{w}}_1 = \mathbf{U}_s\mathbf{\Lambda}_s^{-1}\mathbf{U}_s^H\tilde{\mathbf{P}}\left(\tilde{\mathbf{P}}^H\mathbf{U}_s\mathbf{\Lambda}_s^{-1}\mathbf{U}_s^H\tilde{\mathbf{P}}\right)^{-1}\mathbf{1}_1. \tag{16}$$

For the group-blind MUD of (16), the interfering signals arriving from *known* intracell users are nulled by a projection of the received signal onto the orthogonal subspace of these users' signal subspace. The unknown interfering users' signals inflicted by other cell users are suppressed by identifying the subspace spanned by these intercell users, followed by a linear transformation in this subspace based on the MMSE criterion.

V. Subspace-Tracking Algorithms

The classic approach to subspace-based channel and/or data estimation is centered around the aforementioned EVD of the sample autocorrelation matrix $\mathbf{R}$ or the singular value decomposition (SVD) of the data matrix. However, both the EVD and the SVD exhibit a high complexity since the number of operations to be carried out is on the order of $O[(2NVM)^3]$ in the proposed smart-antenna-aided generalized MC DS-CDMA system, which becomes particularly problematic in agile adaptive applications. In practical scenarios, we are interested in efficient subspace-tracking algorithms, which are capable of recursively updating the subspace on a sample-by-sample fashion.

A. PASTd Algorithm

The PASTd algorithm [3], [14] was first proposed by Yang for the sake of recursively tracking the signal subspace. This algorithm is capable of almost guaranteed global convergence to the true eigenvectors and eigenvalues of the received signal at a low computational complexity, which is on the order of $O(2NVM \cdot J)$ in our system.

TABLE I
PASTd Algorithm Designed for Tracking the Signal Subspace Components of the Received Signal Vector $\mathbf{r}$

Operational procedure of the PASTd algorithm Updating the eigenvalues and eigenvectors of signal space $\lambda_j, \mathbf{u}_j$.
$\mathbf{x}_1(n) = \mathbf{r}(n)$
FOR $j = 1 : J$ DO
$y_j(n) = \mathbf{u}_j^H(n-1)\mathbf{x}_j(n)$; projection operation
$\lambda_j(n) = \beta\lambda_j(n-1) + \lvert y_j(n)\rvert^2$; updating eigenvalue
$\mathbf{u}_j(n) = \mathbf{u}_j(n-1) + \frac{[\mathbf{x}_j(n) - \mathbf{u}_j(n-1)y_j(n)]y_j^*(n)}{\lambda_j(n)}$; updating eigenvectors
$\mathbf{x}_{j+1}(n) = \mathbf{x}_j(n) - \mathbf{u}_j(n)y_j(n)$;
END
$\sigma^2(n) = \beta\sigma^2(n-1) + \frac{\lVert\mathbf{x}_{J+1}(n)\rVert^2}{N-J}$; updating noise variance

The PASTd algorithm in [3] and [14], which is designed for signal subspace tracking, is summarized in Table I, where $\mathbf{r}(n)$ is the nth J-component received signal sample vector, and $\lambda_j(n)$ and $\mathbf{u}_j(n)$ represent the jth eigenvalue and jth eigenvector at the nth time instant, respectively. Finally, $\sigma^2(n)$ is the vector of noise variance during the nth time instant. Table I summarizes the operations of the PASTd algorithm, which is based on the so-called deflation technique [14], and its basic philosophy is that of the sequential estimation of the so-called principal components [14]. The most dominant eigenvector is first updated by applying the PASTd algorithm during the first iteration [14]. Then, the projection of the current signal sample vector $\mathbf{r}(n)$ onto this eigenvector is removed from $\mathbf{r}(n)$ itself. Now, the second most dominant eigenvector becomes the most dominant eigenvector in the updated signal sample vector and can be extracted the same way as before. This procedure is repeatedly applied until all desired eigencomponents have been estimated.

B. NAHJ-FST Algorithm

As described in Section V-A, the PASTd algorithm uses the iterative deflation technique in [14] to sequentially estimate the principal components, commencing with the largest eigenvalues and eigenvectors. The accumulation of the roundoff estimation errors imposed by this procedure may, however, lead to poor estimates of the highly attenuated low-power signals' eigenvalues and their corresponding eigenvectors. Furthermore, the blind and group-blind MUDs in [3], [4], and [9] require the inversion of the signals' eigenvalues, which exacerbates the effect of estimation errors on the low-power signals' eigenvalues, resulting in a degraded output SINR.

The NAHJ-FST algorithm proposed in [15] employs the well-known symmetric Jacobian SVD algorithm [16] for the diagonalization of the autocorrelation matrix $\mathbf{R}$. More explicitly, the NAHJ-FST algorithm invokes a series of Givens rotations [15], [16] to diagnose matrix $\mathbf{R}$. After a number of Givens rotation operations, the autocorrelation matrix $\mathbf{R}$ becomes a *near* diagonal matrix $\mathbf{R}_a$, whose diagonal elements may be viewed as the corresponding eigenvalues; the result of a series of Givens rotations may be viewed as the corresponding eigenvectors. The operation of the NAHJ-FST algorithm invoked for the smart-antenna-aided generalized MC DS-CDMA system considered is summarized in Table II, where γ is the forgetting factor. Note that the NAHJ-FST algorithm employed also exhibits a low complexity that is on the order of $O(2NVM \cdot J)$.

VI. Performance Result

All the investigations in this section were based on the evaluation of the performance of the subspace-based blind and group-blind MUDs employed in the uplink of the smart-antenna-aided generalized

TABLE II
NAHJ-FST ALGORITHM FOR FAST TRACKING THE SIGNAL SUBSPACE COMPONENTS OF THE RECEIVED SIGNAL VECTOR $\mathbf{r}$

Operation procedure of NAHJ-FST algorithm Updating the eigenvalues and eigenvectors of signal space $\mathbf{\Lambda}_s, \mathbf{U}_s$.
1. Projecting the received signal vector $\mathbf{r}(l+1)$ to signal subspace: $\mathbf{r}_s = \mathbf{U}_s^H(l)\mathbf{r}(l+1)$, Generating $\beta = \|\mathbf{r}(l+1) - \mathbf{U}_s(l)\mathbf{r}_s\|$ and the noise-average vector $\mathbf{u}_n = \frac{\mathbf{r}(l+1)-\mathbf{U}_s(l)\mathbf{r}_s}{\beta}$; 2. Generating $\mathbf{R}_s = \left(\begin{bmatrix} \gamma\mathbf{\Lambda}_s^2(l) & 0 \\ 0 & \gamma\sigma^2(l) \end{bmatrix} + [[\mathbf{r}_s^H\|\beta]^H[\mathbf{r}_s^H\|\beta]] \right)$; 3. Diagonalizing the matrix $\mathbf{R}_s$ to $\mathbf{R}_a$ with $r+1$ Givens rotations: $\mathbf{R}_a = \Theta_{r+1}^T \ldots \Theta_1^T \mathbf{R}_s \Theta_1 \ldots \Theta_{r+1}$; 4. Let $\mathbf{\Lambda}_s(l+1)$ be the diagonal matrix whose diagonal elements is equal to the largest r elements of the diagonal elements of $\mathbf{R}_a$; 5. Updating $\mathbf{\Lambda}_s^2(l+1)$ to be the $r+1$ principal submatrix of $\mathbf{R}_a$. 6. Updating $\mathbf{U}_s(l+1)$ to be the first $r+1$ columns of $\begin{bmatrix} \mathbf{U}_s(l+1) \\ \mathbf{u}_n \end{bmatrix} = \begin{bmatrix} \mathbf{U}_s(l) \\ \mathbf{u}_n \end{bmatrix} \Theta_1 \ldots \Theta_{r+1}$; 7. Reaveraging the noise power: $\sigma^2(l+1) = \frac{(N-r-1)(\sqrt{\gamma}\sigma^2(l))+\hat{\sigma}^2}{N-r}$, where $\hat{\sigma}^2 = [\mathbf{R}_a]_{r+1,r+1}$.

TABLE III
BASIC SIMULATION PARAMETERS FOR THE BLIND AND GROUP-BLIND MUDS INVOKED FOR THE GENERALIZED MC DS-CDMA UPLINK

Parameters	Value
Chips-spaced CIR length L	3
Normalized Dopper frequency	0.01
Short cyclic prefix	2 chips
Burst length M_F	256
Number of subcarriers V	4
FD Spreading gain	4
TD Spreading gain	15

MC DS-CDMA system when communicating over a dispersive ST Rayleigh fading channel contaminated by AWGN. An antenna array having M number of AEs is considered in our investigations. When the AEs are located sufficiently far apart, the MC DS-CDMA signal experiences independent fading upon reaching the different AEs; hence, we have the cross-correlation coefficient $\rho = 0$ among the AEs. By contrast, when the AEs are separated by a distance of half a wavelength, we have $\rho = 1$, which implies that these AEs are fully correlated. The basic parameters of the blind and group-blind MUDs invoked for the generalized MC DS-CDMA system considered are summarized in Table III.

In Fig. 2(a) and (b), the PASTd algorithm discussed in Section V-A and the NAHJ-FST algorithm presented in Section V-B were invoked for both blind and group-blind MUDs in the context of generalized MC DS-CDMA. Fig. 2(a) demonstrated that the MUDs employing the PASTd algorithm converged to their steady-state solutions in approximately 800 iterations, corresponding to 800 MC DS-CDMA symbols. Furthermore, the group-blind MUD significantly outperforms the blind MUD. For example, when we supported a total of $K = 5$ users and the signature sequences of $\tilde{K} = 4$ intracell users were known, the group-blind MUD had an output signal-to-interference-plus-noise ratio (SINR) that is higher by 3 dB than that of the blind MUD. By contrast, in Fig. 2(b), the NAHJ-FST algorithm converged after receiving approximately 200 symbols, substantially outperforming the PASTd algorithm characterized in Fig. 2(a). Furthermore, the NAHJ-FST tracking algorithm shown in Fig. 2(a) exhibited a better steady-state performance than that of the PASTd tracking algorithm shown in Fig. 2(a).

In Fig. 3(a), three different types of antenna arrays, i.e., a single antenna and an array having $M = 2$ correlated AEs or $M = 2$

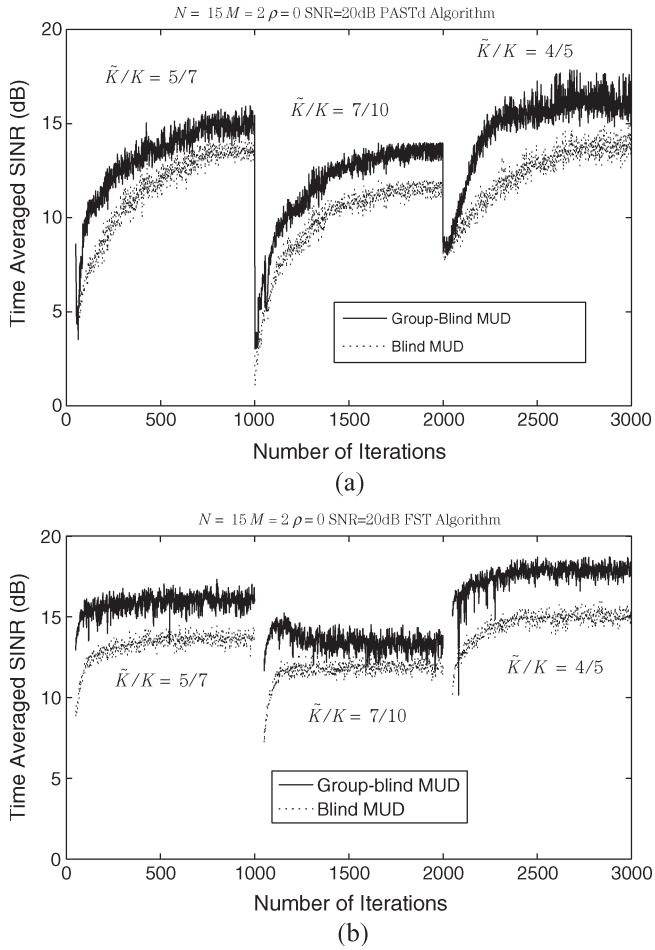

Fig. 2. Performance of both the blind and group-blind MUDs presented in Section IV over a dispersive ST Rayleigh fading channel at an SNR of 20 dB using $M = 2$ uncorrelated AEs and $\rho = 0$. At $t = 0$, $K = 7$ users are activated, and we have $\tilde{K} = 5$ intracell users. At $t = 1000$ iterations, i.e., 1000 symbols, three more users are activated; hence, we have $K = 10$ and $\tilde{K} = 7$. Finally, at $t = 2000$, five users exit the system; hence, we have $K = 5$, as well as $\tilde{K} = 4$. The forgetting factor is 0.995. The curves plotted are averaged over 100 simulation runs, and the remaining parameters are summarized in Table III. (a) PASTd algorithm. (b) NAHJ-FST algorithm.

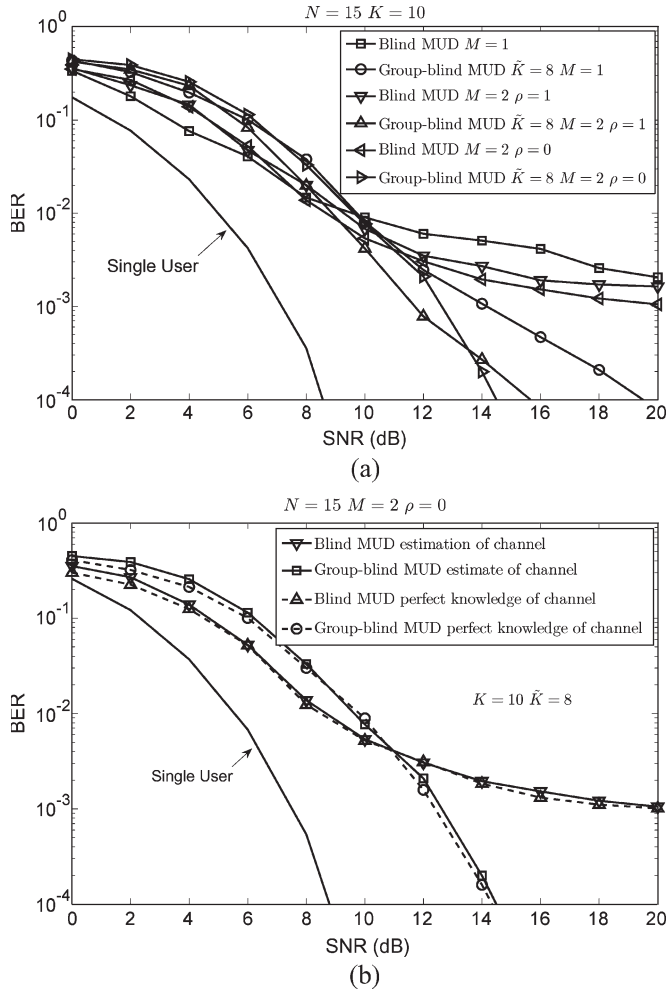

Fig. 3. BER performance for $K = 10$ users, where the group-blind MUDs benefited from the knowledge of $\tilde{K} = 8$ intracell users' spreading codes. The system parameters in Table III were used. (a) Both a single antenna and $M = 2$ correlated and uncorrelated AEs were used. (b) $M = 2$ uncorrelated AEs, $\rho = 0$, and both perfect and realistic blind channel estimations were considered.

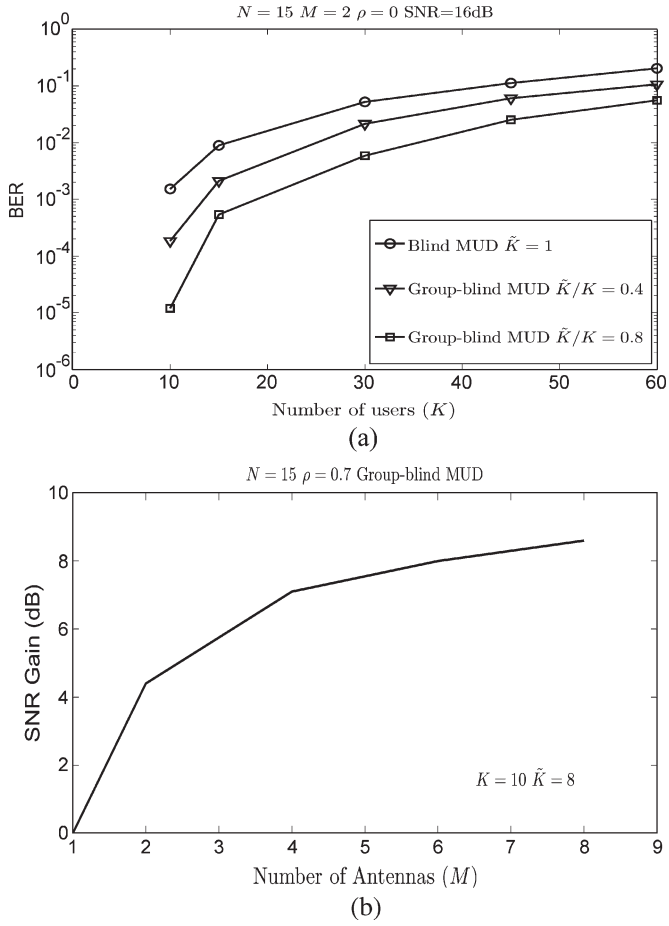

Fig. 4. (a) Plot of BER versus the number of users K for the various MC DS-CDMA MUDs considered. An antenna array having $M = 2$ uncorrelated AEs was employed, and we had $\rho = 0$. The SNR was fixed at 16 dB. For the group-blind MUDs, we had $\tilde{K}/K = 0.4$ or 0.8. (b) Plot of the SNR gain versus M for the group-blind MUDs at a BER of 10^{-4}. Antenna arrays having a cross-correlation coefficient of $\rho = 0.7$ were used, and $K = 10$ users were supported. The group-blind MUDs benefited from the knowledge of the spreading codes of $\tilde{K} = 8$ intracell users. The remaining system parameters are summarized in Table III.

uncorrelated AEs, were employed. The simulation results showed that the group-blind MUD benefiting from the knowledge of the signature waveforms of more intracell users attained a better bit error rate (BER) performance in the high-SNR region. Furthermore, Fig. 3(a) demonstrated that, as expected, the blind MUD operating in conjunction with an antenna array having $M = 2$ uncorrelated AEs achieved a better BER performance than that having $M = 2$ correlated AEs. The blind MUD employing a single antenna attained the worst BER performance. In Fig. 3(b), we observe that the blind and group-blind ST MUDs equipped with the subspace-based CIR estimator perform only slightly worse than the estimator exploiting the perfect knowledge of the CIRs, which implies that the associated performance degradation imposed by the channel estimator error is negligible.

In Fig. 4(a), an antenna array having $M = 2$ uncorrelated AEs was employed, and we had $\rho = 0$, where the BER performance of the blind and group-blind MUDs was presented as a function of the number of users supported. Note that the system having $V = 4$ and $N = 15$ and, hence, the capability of serving $K = 60$ users was fully loaded. Finally, Fig. 4(b) characterizes the SNR gains achieved by increasing the number of AEs, demonstrating that increasing the number of AEs can provide an increased degree of freedom and, hence, substantially improve the attainable system performance at the expense of a higher system complexity.

VII. Conclusion

It was demonstrated that the NAHJ-FST tracking algorithm exhibited faster convergence and better steady-state performance than the PASTd tracking algorithm. As expected, the group-blind MUD, which benefited from the knowledge of the signature waveforms of more intracell users, attained a better BER performance in the high-SNR region. The blind and group-blind ST MUDs equipped with the subspace-based CIR estimator perform only slightly worse than the estimator exploiting the perfect knowledge of the CIRs, which implied that the performance degradation imposed by the blind—rather than trained—channel estimator is negligible. Our simulation results suggested that increasing the number of AEs can provide an increased degree of freedom and, hence, substantially improve the attainable performance at the expense of a higher system complexity. Furthermore, employing more subcarriers will increase the attainable frequency diversity gain and, hence, improve the achievable performance at the cost of an increased system complexity. When employing a single antenna, the group-blind MUD that benefits from the knowledge of the signature waveforms of $\tilde{K} = 8$ intracell users, and, hence, carries out blind channel estimation for these $\tilde{K} = 8$ users, outperformed the totally blind MUD by 2.9 dB at a BER of 5×10^{-3} since the

latter MUD exploited the signature waveform of the desired user only. When employing the NAHJ-FST algorithm, the group-blind MUD employing an antenna array having $M = 2$ AEs exposed to uncorrelated fading achieved a 4.2-dB SNR gain at a BER of 10^{-4} compared with that employing a single antenna, which was a benefit of increasing the computational complexity from the order of $O(2NV \cdot J)$ to $O(4NV \cdot J)$.

REFERENCES

[1] S. Verdu, *Multiuser Detection*. Cambridge, U.K.: Cambridge Univ. Press, 1998. 474 pp.

[2] M. Honig, U. Madhow, and S. Verdu, "Blind adaptive multiuser detection," *IEEE Trans. Inf. Theory*, vol. 41, no. 4, pp. 944–960, Jul. 1995.

[3] X. Wang and H. V. Poor, "Blind multiuser detection: A subspace approach," *IEEE Trans. Inf. Theory*, vol. 44, no. 2, pp. 677–690, Mar. 1998.

[4] X. Wang and A. Host-Madsen, "Group-blind multiuser detection for uplink CDMA," *IEEE J. Sel. Areas Commun.*, vol. 17, no. 11, pp. 1971–1984, Nov. 1999.

[5] L. Hanzo, L. L. Yang, E. L. Kuan, and K. Yen, *Single- and Multi-Carrier DS-CDMA*. New York: Wiley, 2003. 1060 pp.

[6] D. S. Chen and S. Roy, "An adaptive multiuser receiver for CDMA systems," *IEEE J. Sel. Areas Commun.*, vol. 12, no. 5, pp. 808–816, Jun. 1994.

[7] G. Woodward and B. S. Vucetic, "Adaptive detection for DS-CDMA," *Proc. IEEE*, vol. 86, no. 7, pp. 1413–1434, Jul. 1998.

[8] U. Madhow, "MMSE interference suppression for timing acquisition and demodulation in direct-sequence CDMA systems," *IEEE Trans. Commun.*, vol. 46, no. 8, pp. 1065–1075, Aug. 1998.

[9] X. Wang and H. V. Poor, "Blind equalization and multiuser detection in dispersive CDMA channels," *IEEE Trans. Commun.*, vol. 46, no. 1, pp. 91–103, Jan. 1998.

[10] J. Namgoong, T. F. Wong, and J. S. Lehnert, "Subspace multiuser detection for multicarrier DS-CDMA," *IEEE Trans. Commun.*, vol. 48, no. 11, pp. 1897–1908, Nov. 2000.

[11] L.-L. Yang and L. Hanzo, "Performance of generalized multicarrier DS-CDMA over Nakagami-m fading channels," *IEEE Trans. Commun.*, vol. 50, no. 6, pp. 956–966, Jun. 2002.

[12] L. Hanzo, M. Munster, B. J. Choi, and T. Keller, *OFDM and MC-CDMA*. New York: Wiley, 2003. 960 pp.

[13] S. Zhou, B. Muquet, and G. B. Giannakis, "Subspace-based (semi-) blind channel estimation for block precoded space-time OFDM," *IEEE Trans. Signal Process.*, vol. 50, no. 5, pp. 1215–1228, May 2002.

[14] B. Yang, "Projection approximation subspace tracking," *IEEE Trans. Signal Process.*, vol. 43, no. 1, pp. 95–107, Jan. 1995.

[15] D. Reynolds and X. Wang, "Adaptive group-blind multiuser detection based on a new subspace tracking algorithm," *IEEE Trans. Commun.*, vol. 49, no. 7, pp. 1135–1141, Jul. 2001.

[16] S. Haykin, *Adaptive Filter Theory*, 3rd ed. Upper Saddle River, NJ: Prentice-Hall, 1996.

Downlink Resource Management in the Frequency Domain for Multicell OFCDM Wireless Networks

Riku Jäntti, *Senior Member, IEEE*, and
Seong-Lyun Kim, *Member, IEEE*

***Abstract*—Recently, various versions of combining code division multiple access (CDMA) with orthogonal frequency-division multiplexing (OFDM) have drawn much attention for IMT-Advanced (4G) and new broadcasting systems. In particular, variable-spreading-factor orthogonal frequency and code multiplexing (OFCDM) and multicarrier CDMA adopt 2-D spreading, i.e., time-domain and frequency-domain spreading. Maeda *et al.*, Yang and Hanzo, Zheng *et al.*, and Zhou *et al.* have mentioned a few strong points of 2-D spreading. However, what is missing in their analysis/simulations is the system-level aspect of 2-D spreading. In particular, we are interested in the following questions: "What are the advantages of frequency-domain spreading in multicell environments?" and "What is the optimal frequency reuse factor in 2-D spreading systems?" Answers to these questions are investigated in this correspondence.**

***Index Terms*—Frequency-domain spreading, frequency reuse factor, orthogonal frequency and code multiplexing (OFCDM), outage probability, 2-D spreading.**

I. INTRODUCTION

In addition to randomizing the other cell interference, one unique feature in second-generation and third-generation (2G and 3G) code-division multiple-access (CDMA) systems is the Rake receiver that effectively catches the multipaths to achieve the so-called path diversity. However, as high data rates are required, the multipath delay becomes greater than the symbol duration. This could result in severe intersymbol interference (ISI), which cannot be completely removed by a finite number of Rake fingers. If the negative effect due to ISI is more dominant than the positive effect from path diversity, the performance in CDMA systems might degrade as the delay spread increases. To mitigate the ISI effect with low complexity, orthogonal frequency-division multiplexing (OFDM) has drawn much attention.

In the meantime, to exploit the advantages of OFDM and CDMA systems, combining these two techniques has been suggested in multicarrier CDMA [1]. In a multicarrier system, we can spread the symbol in two ways. One option is to spread the symbol into a subcarrier so that we can multiplex more than one user's symbols on a subcarrier (time-domain spreading). Another spreading option is to spread the symbol into many subcarriers in parallel (frequency-domain spreading). Thus, the total spreading factor is the multiplication of time-domain and frequency-domain spreading factors. A 2-D spreading orthogonal frequency and code multiplexing (OFCDM) system refers to a system that employs both ways of spreading (see [2]–[5] and the references therein). Examples of 2-D spreading OFCDM can be found in variable spreading factor OFCDM [2] and multicarrier DS-CDMA [3].

Manuscript received November 30, 2006; revised October 14, 2007 and November 12, 2007. The work of S.-L. Kim was supported by the Broadband OFDM Mobile Access Information Technology Research Center (BrOMA-ITRC) of the Korean Ministry of Information and Communication (MIC) under Grant IITA-2007-C1090-0701-0037. The review of this paper was coordinated by Prof. C.-J. Chang.

R. Jäntti is with the Communications Laboratory, Helsinki University of Technology (TKK), 02015 Espoo, Finland (e-mail: riku.jantti@tkk.fi).

S.-L. Kim is with the Radio Resource Management and Optimization Laboratory, School of Electrical and Electronic Engineering, Yonsei University, Seoul 120-749, Korea (e-mail: slkim@yonsei.ac.kr).

Digital Object Identifier 10.1109/TVT.2007.914056